Chemosphere 113 (2014) 158–164

Contents lists available at ScienceDirect

Chemosphere

journal homepage: www.elsevier.com/locate/chemosphere

Novel insights into anoxic/aerobic^1/aerobic^2 biological fluidized-bed system for coke wastewater treatment by fluorescence excitation–emission matrix spectra coupled with parallel factor analysis

Hua-Se Ou [a,b,*], Chao-Hai Wei [b], Ce-Hui Mo [a], Hai-Zhen Wu [b], Yuan Ren [b], Chun-Hua Feng [b]

[a] Department of Environmental Engineering, Jinan University, Guangzhou 510632, PR China
[b] The Key Lab of Pollution Control and Ecosystem Restoration in Industry Clusters, Ministry of Education, College of Environment and Energy, South China University of Technology, Higher Education Mega Center, Guangzhou 510006, PR China

HIGHLIGHTS

- We developed a novel anoxic/aerobic^1/aerobic^2 process to treat coke wastewater.
- DOM in bio-treatment was characterized using EEM and PARAFAC.
- Correlations between contaminants and EEM components were investigated.
- EEM–PARAFAC can be used to monitor the performance of coke wastewater treatment.

GRAPHICAL ABSTRACT

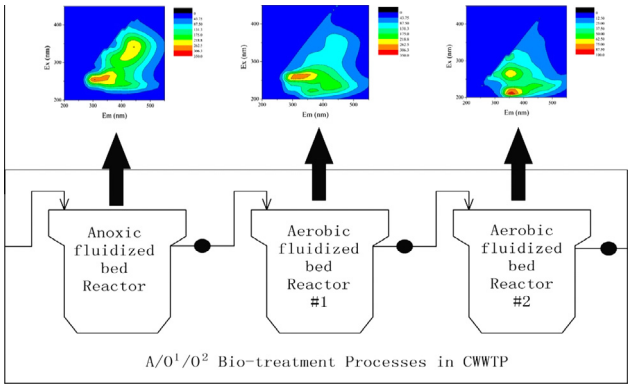

ARTICLE INFO

Article history:
Received 11 January 2014
Received in revised form 23 April 2014
Accepted 25 April 2014
Available online 29 May 2014

Handling Editor: O. Hao

Keywords:
Chromophoric dissolved organic matter
Phenol
Cyanide
Coke wastewater
Parallel factor analysis
Principal component analysis

ABSTRACT

Fluorescence spectroscopy coupled with parallel factor analysis (PARAFAC) was applied to investigate the contaminant removal efficiency and fluorescent characteristic variations in a full scale coke wastewater (CWW) treatment plant with a novel anoxic/aerobic^1/aerobic^2 (A/O^1/O^2) process, which combined with internal-loop fluidized-bed reactor. Routine monitoring results indicated that primary contaminants in CWW, such as phenols and free cyanide, were removed efficiently in A/O^1/O^2 process (removal efficiency reached 99% and 95%, respectively). Three-dimensional excitation–emission matrix fluorescence spectroscopy and PARAFAC identified three fluorescent components, including two humic-like fluorescence components (C1 and C3) and one protein-like component (C2). Principal component analysis revealed that C1 and C2 correlated with COD (correlation coefficient (r) = 0.782, $p < 0.01$ and $r = 0.921$, $p < 0.01$), respectively) and phenols ($r = 0.796$, $p < 0.01$ and $r = 0.914$, $p < 0.01$, respectively), suggesting that C1 and C2 might be associated with the predominating aromatic contaminants in CWW. C3 correlated with mixed liquor suspended solids ($r = 0.863$, $p < 0.01$) in fluidized-bed reactors, suggesting that it might represent the biological dissolved organic matter. In A/O^1/O^2 process, the fluorescence intensities of C1 and C2 consecutively decreased, indicating the degradation of aromatic contaminants. Correspondingly, the fluorescence intensity of C3 increased in aerobic^1 stage, suggesting an increase of biological dissolved organic matter.

* Corresponding author at: Guangzhou Higher Education Mega Centre, Panyu District, Guangzhou, CN 510006, PR China. Tel.: +86 020 87112874.
E-mail address: ouhuase@126.com (H.-S. Ou).

http://dx.doi.org/10.1016/j.chemosphere.2014.04.102
0045-6535/

1. Introduction

460 Mt coke in China, important raw material for steelmaking, was yielded in 2012. Coke wastewater (CWW) is one of the harmful by-products of coke production, which contains considerable amounts of phenols, polycyclic aromatic hydrocarbons (PAHs), heterocyclic compounds (HCs), cyanide, and sulfide compounds. It has been reported that ~24.0 kt of phenols, ~0.7 kt of cyanide and 1.6 kt of benzo[a]pyrene were discharged from CWW in China in 2005 (NDRC, 2006). These compounds were recognized as carcinogenic, mutagenic and toxic contaminants, which were listed as US-EPA and EU priority pollutants (Angelino and Gennaro, 1997). Therefore, it was essential to efficiently remove these contaminants in CWW to reduce their hazard to aquatic organisms and humans.

The activated sludge process was indisputably the most frequently employed biological technique in CWW treatment plants (CWWTPs). In China, the existing CWWTPs mostly used anaerobic/anoxic/aerobic ($A^1/A^2/O$) bio-treatment process with continuously stirred reactors, since this combination was easily designed and operated (Wei et al., 2012). However, good performance in carbon and nitrogen removal was difficult to achieve because of toxic contaminants inhibition on various biological reactions (Staib and Lant, 2007). To solve this problem, worldwide researchers had focused on the development of efficient bio-treatment technique for CWW (Zhang et al., 1998; Maranon et al., 2008). However, most researches were conducted in bench or pilot scale, and only a few new developed techniques were applied in full-scale CWWTPs (Kim et al., 2009). Recently, the Chinese government issued stricter new standard for aqueous discharges of CWW (Ministry of Environmental Protection, 2012). Therefore, it was urgent to develop feasible higher efficient treatment process for Chinese CWWTPs. Based on $A^1/A^2/O$ process, our research group developed a novel anoxic/aerobic^1/aerobic^2 ($A/O^1/O^2$) internal-loop biological fluidized-bed system, which is now successfully applied in a full-scale CWWTP in south China (Zhang et al., 2010).

The phenols, PAHs and HCs in CWW were typical chromophoric dissolved organic matter (CDOM) (Zhang et al., 2013). Meanwhile, the microbial reactions in wastewater bio-treatments generated microbial CDOM (Li et al., 2008). These CDOM can be employed to distinguish the chemical composition of DOM (Hudson et al., 2007), and can provide useful information about the removal efficiency of contaminants. Excitation–emission matrix (EEM) fluorescence spectroscopy was an ideal method to qualitatively characterize CDOM, and the parallel factor analysis (PARAFAC) provided quantitative data about the individual CDOM components (Bro, 1997; Hua et al., 2010). Therefore, EEM–PARAFAC might have potential to rapidly and continuously monitor contaminant removal efficiency in CWWTPs.

To date, only a few researches used fluorescence spectra to describe the characteristic of CWW CDOM in laboratory or pilot scale tests (Zhao et al., 2009; Wei et al., 2012; Yang et al., 2013), but not in full scale CWWTPs. Therefore, this study aimed to describe the characteristics and behaviors of CDOM components in a full scale CWWTP with a novel $A/O^1/O^2$ fluidized-bed system. Qualitative analysis of CDOM was conducted using EEM–PARAFAC, and correlations between CDOM and routine parameters were investigated using statistical analysis.

2. Materials and methods

2.1. CWWTP and data set

The samples were collected from No. 1 Songshan CWWTP, which was located in Shaoguan Steel, Guangdong Province, China, with a designed treatment capacity of 1680 $m^3\ d^{-1}$. Table SM-1 in Supplementary Material (SM) presents the statistical monitoring variables of raw influent. The treatment of this CWWTP included three processes: pretreatment, bio-treatment and advanced treatment (Fig. 1). After pretreatment, the liquid effluent flowed into the bio-treatment processes. One $A/O^1/O^2$ system coupled with three internal-loop biological fluidized-beds in the volumes of 2360, 3280 and 2780 m^3 was applied (Table SM-2). The biological effluent then flowed through advanced treatment and the final effluent was discharged or reused. The water samples were collected from the influent of bio-treatment and the effluent of each stage in $A/O^1/O^2$, and then were stored in 2–4 °C prior to analysis. Sampling was conducted every 3 d from January 1, 2012 to December 31, 2012.

2.2. Analytical methods

The COD, NH_3, pH and MLSS were measured by online COD_{max}-Plus monitors (Hach, USA), by Amtax Compact analyzers (Hach, USA), by online GLI pH/ORP monitors (Hach, USA), and by online Solita SC monitors (Hach, USA), respectively. Other variables were determined at laboratory. Before analysis, the water samples were centrifuged and the supernatant was filtered with 0.7 μm GF/F filter and then 0.2 μm membrane filter (MFS, Japan) to obtain the extracted solution. The concentrations of phenols, sulfide and free cyanide were determined according to Standard Methods (APHA, 1998).

For EEM analysis, the extracted solution was diluted 10 times by ultra-pure water to a COD concentration in the range of 20–257 mg L^{-1}, and then the pH value of diluted solution was adjusted to 7.0 ± 0.1. EEM spectrograms of extracted solution were measured using a Cary Eclipse fluorescence analyzer (Varian Instruments, USA) with a 4 mL, 1 cm path length cuvette. The photomultiplier tubes voltage was set at 600 V, and the slits for both excitation and emission were 5 nm with scanning speed at 1200 nm min^{-1}. The fluorescence region 550 nm > Emission (Em) > 200 nm, 450 nm > Excitation (Ex) > 200 nm was set as the scan region with 5 nm intervals. Replicate scans were generally within 5% agreement in terms of intensity and within the slit width resolution in terms of peak location. Fluorescent intensity was calibrated in quinine sulfate equivalents (QSE), where 1 QSE is the maximum fluorescent intensity of 0.01 mg L^{-1} of quinine in 1 N H_2SO_4 at the Ex/Em = 350 nm/450 nm (Hoge et al., 1995). The Cary Eclipse analyzed samples in default ratio mode. The detailed information about spectra correction steps can be found in previous study (Yao et al., 2011).

2.3. PARAFAC

EEM spectrograms were combined into a 3-dimensional data array: 120 samples × 51 excitations × 71 emissions. Before analysis, the Raman scattering was removed by subtracting the pure water spectrogram from the sample spectrogram. Rayleigh scatter effects were removed from the data set by excluding any emission measurements made at wavelengths ⩽ excitation wavelength +5 nm, and at wavelengths ⩾ excitation wavelength +300 nm. Zero was added to the EEMs in the two triangle regions (emission wavelength ⩽ excitation wavelength +5 nm, and ⩾ excitation wavelength +300 nm) of the missing data (Yao et al., 2011). The PARAFAC analysis was conducted using MATLAB (MathWorksm, USA) to extract CDOM components from EEM fluorescence data. The algorithm used in this work is available from the N-way Toolbox for MATLAB at http://www.models.kvl.dk. After the PARAFAC model was established, core consistency diagnostic and split half analysis were used to validate the models. One sample was removed through comparing it to the others to determine whether

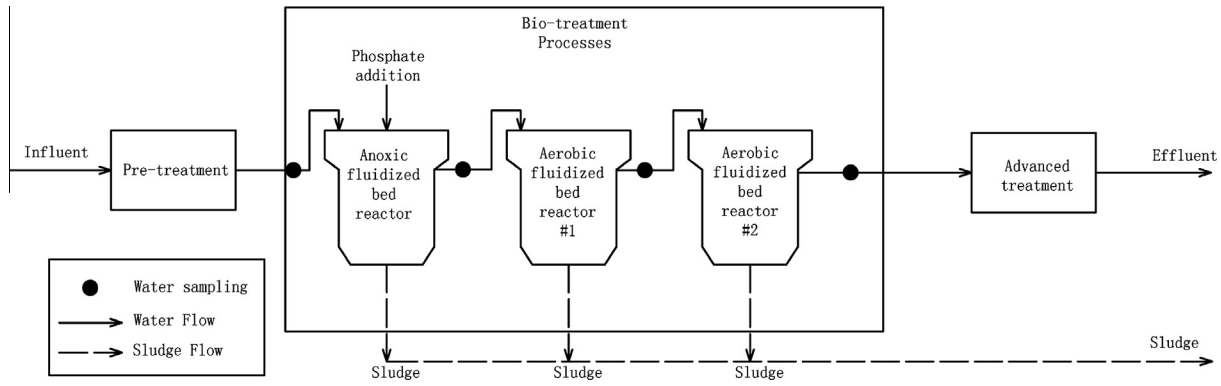

Fig. 1. Schematic diagram of No.1 Songshan coke wastewater treatment plant and sampling sites. The bio-treatment contained an A/O^1/O^2 process with fluidized-bed reactors. The water samples were collected from influent of bio-treatment and effluent of each stage in A/O^1/O^2 from January 1, 2012 to December 31, 2012 (sampling and analysis every 3 d).

it contained measurement error. The PARAFAC model returned only relative intensities of components (scores); thus the intensity of the *n*th component in a given sample, I_n, was calculated using the following equation (Kowalczuk et al., 2009):

$$I_n = Score_n \times \mathrm{Ex}_n(\lambda_{max}) \times \mathrm{Em}_n(\lambda_{max}) \quad (1)$$

where $Score_n$ is the relative intensity of the *n*th component, Ex_n (λ_{max}) is the maximum excitation loading of the *n*th component, and Em_n (λ_{max}) is the maximum emission loading of the *n*th component derived from the model.

2.4. Statistical analyses

The data set for principal component analysis (PCA) and correlation analysis included the fluorescence intensity of three PARAFAC components and seven variables. These heterogeneous variances were first normalized into an interval of (−1, 1) using standardizing program which embedded in SPSS 19.0 statistical software (IBM, USA). The PCA of normalized data set was conducted using SPSS 19.0 (Ou et al., 2013). Correlation analyses were conducted using SPSS 19.0 software. The correlation significance was tested using two-way ANOVA.

3. Results and discussion

3.1. Variations of multiple variables

The COD decreased from $(2.99 \pm 0.50) \times 10^3$ to $(2.54 \pm 0.48) \times 10^3$ mg L^{-1} after anoxic stage; then it decreased to 288 ± 91 mg L^{-1} after aerobic^1 stage (Fig. 2). Similar variation tendencies were observed in the results of phenols and sulfide. The concentration of free cyanide decreased from 18 ± 1 to 4 ± 1 mg L^{-1} after anoxic stage. Slight decreases of free cyanide were observed in aerobic^1 and aerobic^2 stages. After bio-treatment, approximate 92% COD, 99% phenols, 95% free cyanide and 81% sulfide were removed. The NH_3 increased from 55 ± 16 to 70 ± 19 mg L^{-1} after aerobic^1 stages, and it decreased to 10 ± 6 mg L^{-1} after aerobic^2 stage. The degradation of free cyanide and other nitrogenous compounds might contribute to the increase of NH_3 in anoxic and aerobic^1 bio-treatments (Akcil et al., 2003). And then the nitrification in aerobic^2 reactor resulted in consumption of NH_3. The MLSS ($(1.91 \pm 0.25) \times 10^3$ mg L^{-1}) increased to $(3.90 \pm 0.30) \times 10^3$ mg L^{-1} in aerobic^1 reactor, and it decreased to $(2.54 \pm 0.25) \times 10^3$ mg L^{-1} in aerobic^2 reactor. Of note, the average pH decreased from 9 to 7 after bio-treatment. The microbial reactions, e.g. nitrification of NH_3, contributed to the variation of pH value.

3.2. EEM spectroscopy characteristics

The EEM spectra of CWW influent and A/O^1/O^2 treated effluent are presented in Fig. 3. Five fluorescence peaks, including T_1, T_2, *B*, *A* and *C*, were identified. In natural surface water, Peak *B* (Ex/Em = 275/310 nm) related to aromatic proteins-like substance (Baker et al., 2003); Peak T_1 (Ex/Em = 275/340 nm) and Peak T_2 (Ex/Em = 210/340 nm) related to soluble microbial by-product-like substance (Coble, 1996); Peaks *C* (Ex/Em = 350/420–480 nm) and *A* (Ex/Em = 260/380–460 nm) related to humic acid- and fulvic acid-like substances derived from the breakdown of plant material (Mounier et al., 1999). As depicted in Fig. 3, the CWW influent had significant Peaks *B* and *C*. These two peaks successively decreased as the bio-treatment proceeded. In contrary, the fluorescent intensities of Peaks T_1, T_2 and *A* increased after A/O^1/O^2 treatment. According to the multiple variables results in Section 3.1, it can be concluded that the fluorescent substances related to these five peaks in CWW were different from those in natural surface water. Peaks *B* and *C* might represent the aromatic matters, such as phenols, benzene and their derivatives. These substances were degraded by microbial reactions in A/O^1/O^2 fluidized bed system. Peaks T_1, T_2 and *A* might relate to the microorganism derived matters. Peaks T_1 and T_2 represented the soluble microbial by-product materials, and Peak *A* represented the debris of the microorganism.

3.3. PARAFAC

PARAFAC modeling of the water samples revealed that the EEM of CWW CDOM could be characterized by three different fractions (Fig. 4). The C1 component had two peaks at Ex/Em = 250/450 nm and at Ex/Em = 345/450 nm. The spectral feature of these peaks was identified as the mixture of HCs and PAHs, such as the fluoranthene (Ex/Em = 287/459 nm), naphthol (330/472 nm) and quinolone (310–340/380–440 nm) (Bridges and Williams, 1968; Burich et al., 1974).

The C2 component had one peak at Ex/Em = 280/320 nm. The fluorescent component emerged from this peak originated from both phenol-like matter and protein-like matter (Wu et al., 2011). The characteristic fluorescent peaks of phenol (271/295 nm) and various PAHs, such as naphthalene (265/336 nm), cresol (270/300 nm) and other derivatives, all located at this region (Alarcón et al., 2012; Lu et al., 2013). Therefore, the C1 and C2 components reflected the mixture of phenols, HCs, PAHs and their derivatives in CWW.

The C3 component was characterized by two peaks at Ex/Em = 230/380 nm and at Ex/Em = 300/380 nm. Compared with

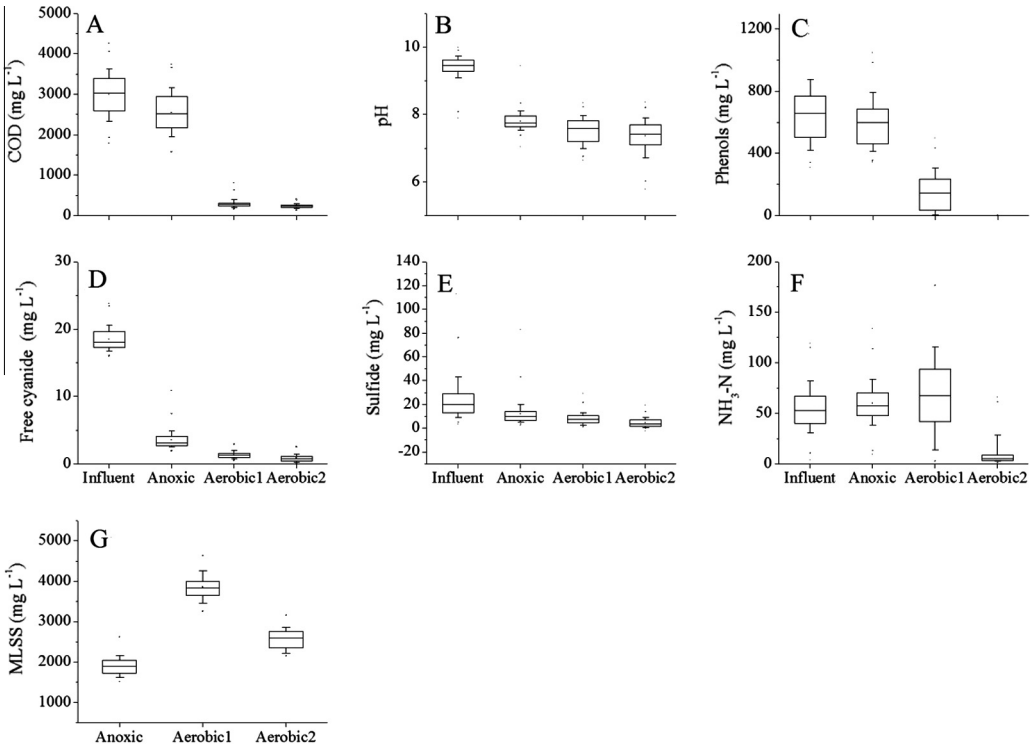

Fig. 2. Variations of multiple variables in A/O^1/O^2 fluidized bed system. Influent indicated the influent of bio-treatment. (A) COD, (B) pH, (C) phenols, (D) free cyanide, (E) sulfide, (F) NH_3-N and (G) MLSS.

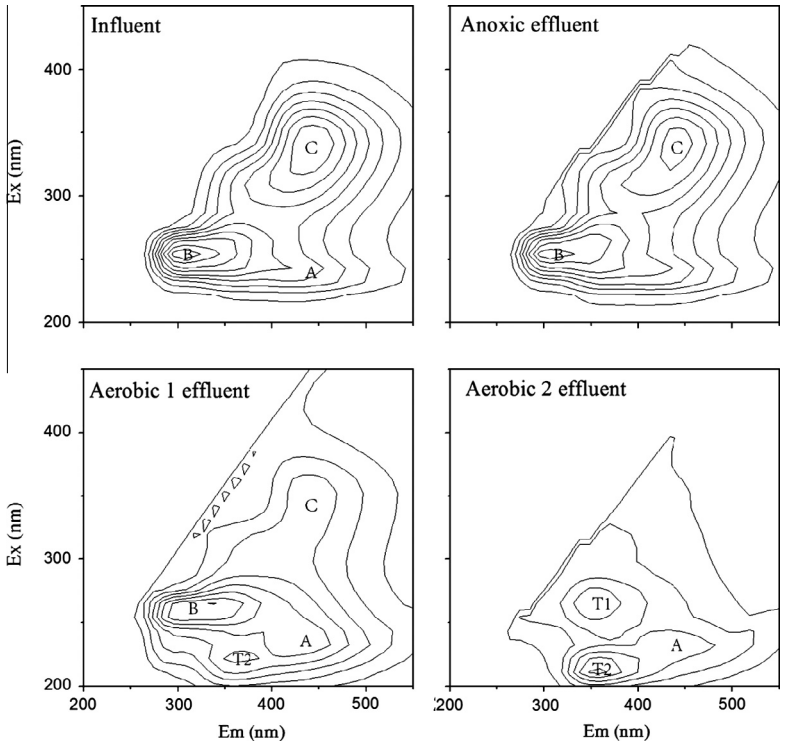

Fig. 3. Excitation-emission-matrix (EEM) spectra of influent and A/O^1/O^2 effluent. The typical fluorescent characteristic peaks were marked as A, B, C, T1 and T2 in the figures. The interval between two lines was 50 QSE.

protein-like matter, the C3 component was more possibly originated from fulvic-like substance (Wu et al., 2011). These two peaks were categorized as the mixture of biological matters in PARAFAC analysis (Li et al., 2008). Therefore, these components might be the microbial derived DOM from biomass.

3.4. Variations of fluorescence intensity of CDOM components

The quantitative analysis of fluorescent component was also conducted by PARAFAC (Fig. 5). The fluorescence intensities of PARAFAC components were calculated according to Eq. (1). The

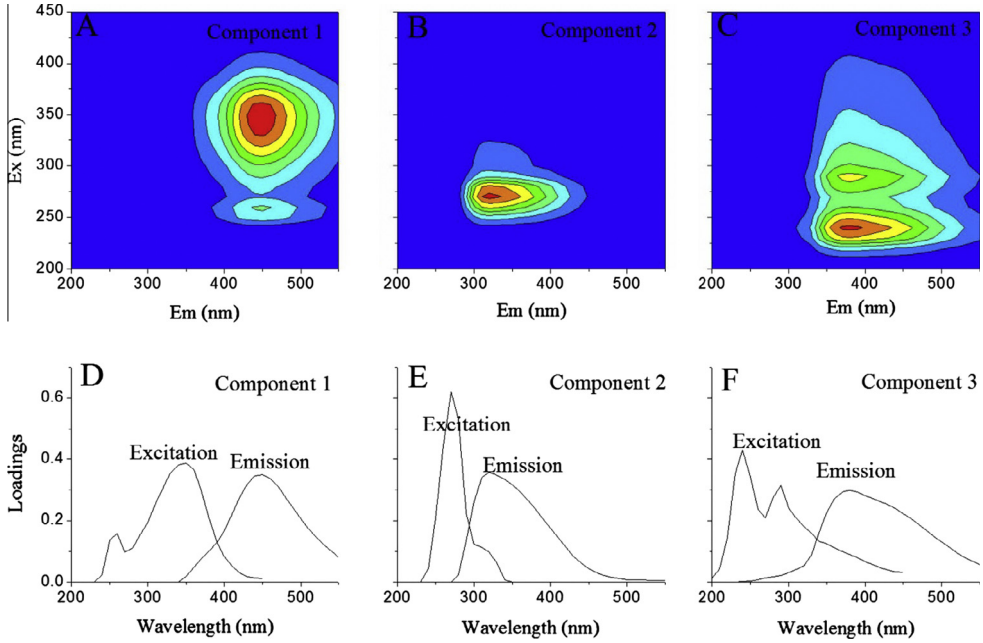

Fig. 4. Three parallel factor (PARAFAC) identified components and their loadings. (A–C) contour plots of the spectral shapes of each component, (D–F) line plots of the loadings of each component.

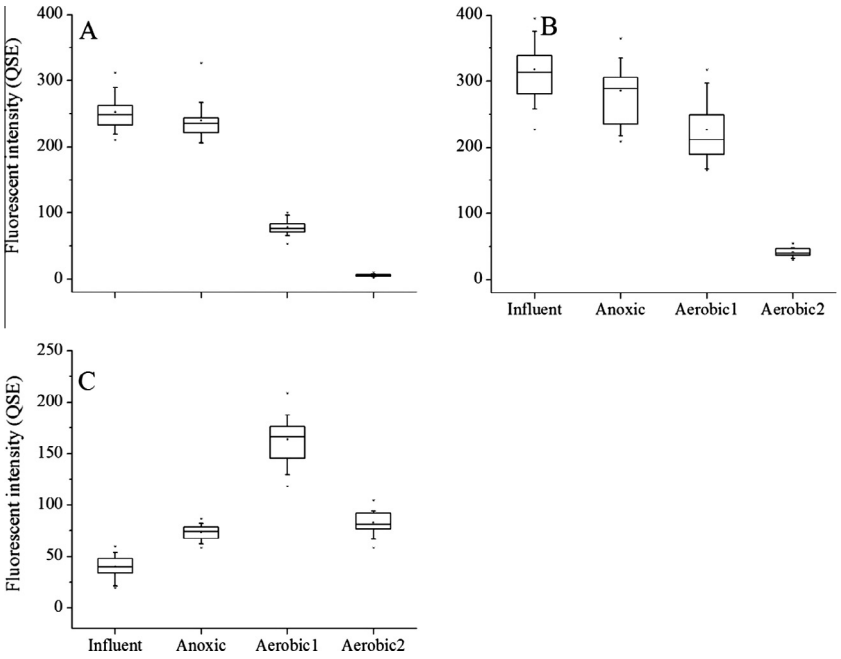

Fig. 5. Fluorescence intensity of PARAFAC components for water samples in $A/O_1/O_2$ fluidized bed process. Influent indicated the influent of bio-treatment. (A) C1, (B) C2 and (C) C3.

intensity of C1 decreased from 252 ± 31 to 6 ± 3 QSE as the bio-treatment proceeded. Similarly, the average intensity of C2 gradually decreased from 317 ± 23 to 226 ± 16 QSE after anoxic and aerobic[1] treatments, and then rapidly decreased to 41 ± 3 QSE after aerobic[2] treatment. In contrary, the intensity of C3 increased from 40 ± 11 to 164 ± 24 QSE after anoxic and aerobic[1] treatments, and then decreased to 83 ± 15 QSE after aerobic[2] treatment. Reductions of the C1 and C2 fluorescence intensities after the $A/O^1/O^2$ treatment indicated the degradation of phenols, HCs, PAHs and their derivatives, and such outcomes were in good agreement with the high removal efficiency of COD and phenols in the Section 3.1. Significant correlations were also observed between C1, C2, COD and phenols (Table SM-3). The increase of C3 fluorescence intensity indicated the generation of biological DOM during anoxic and aerobic[1] treatments, but it decreased in aerobic[2] treatment. The variation tendency of C3 was also in good agreement with MLSS. This result indicated that the fluorescence intensity of CDOM component might assess the variation tendency of contaminant removal and biomass in bio-treatment of CWW.

3.5. PCA

PCA was used to assess the internal correlations between PARAFAC components and other variables. Analytical data set covered

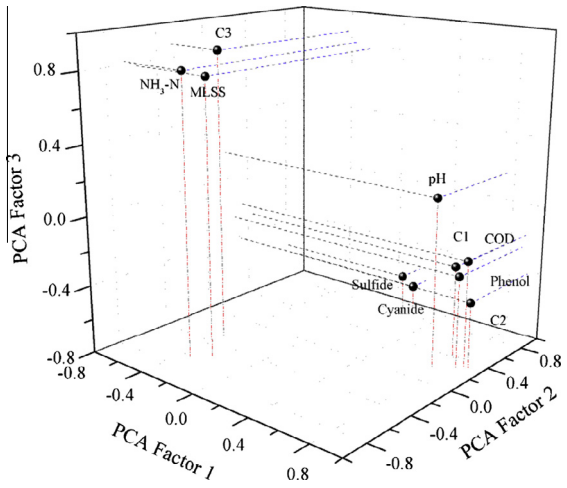

Fig. 6. 3-D PCA loadings scatter diagram of all three factors. The Factor 1, 2 and 3 groups indicated the variables which had high Factor 1, 2 and 3 loadings, respectively.

the fluorescence intensities of three PARAFAC components and seven variables, including COD, phenols, NH_3, free cyanide, sulfide, pH and MLSS. Two key parameters, including eigenvalue and loading, were automatically obtained during PCA calculation. The eigenvalue reflected the dominating level of a component (factor), and the loadings reflected how the variables related to each other in a component (factor). The PCA results indicated that the first three axes (Factors 1, 2 and 3) accounted for 46%, 24% and 17%, respectively, of the variance in all variable distributions (Table SM-4). Fig. 6 presents the PCA factor loadings.

Factor 1 showed closely positive correlations with C2, COD and phenols (loadings at 0.92, 0.87 and 0.89, respectively), while loose correlations with C1 and pH (loadings at 0.79 and 0.76, respectively). There was a close relationship between COD and phenols ($r = 0.869$, $p < 0.01$, Table SM-3), indicating that phenols were representative components in CWW. COD had close correlations with C1 ($r = 0.782$ ($p < 0.01$) and C2 ($r = 0.921$ ($p < 0.01$)), revealing that C1 and C2 might represent the mixture of phenols, HCs, PAHs and their derivatives. Therefore, these two fluorescent components can be used as indicators to monitor the variations of aromatic contaminants.

Factor 2 showed close positive correlations with free cyanide and sulfide (loadings at 0.85 and 0.79, respectively, SM-4), indirectly proved that free cyanide and sulfide had significant correlation ($r = 0.875$ ($p < 0.01$), Table S3). Therefore, PCA Factor 2 can be explained as a complicated parameter which mainly represented the inorganic contaminants (free cyanide and sulfide) in CWW. However, weak correlations between fluorescent components and these two contaminants were observed.

MLSS and fluorescent component C3 showed significant positive PCA Factor 3 loadings (0.79 and 0.88, respectively), and NH_3 had a weaker loading (0.67). MLSS represented the biomass in a reactor, and C3 was identified as the biological fluorescent materials. The correlation between MLSS and C3 was significant ($r = 0.863$ ($p < 0.01$)), indicating the C3 might be generated by the microorganisms in fluidized bed reactors. Therefore, PCA Factor 3 can be explained as a complicated parameter which mainly represented the biomass.

4. Conclusions

CWW contained distinct CDOM, which was different from natural water body. Three CDOM components were identified from CWW by EEM–PARAFAC. According to PCA and correlation results, C1 and C2 might be associated with phenols, HCs, PAHs and their derivatives, and they can be used as indicators of aromatic contaminants. C3 was related to microbial fluorescent materials, and it can be used as an indirect indicator of biomass. These results indicated that EEM–PARAFAC not only can rapidly identify fluorescent matter characteristics, but also can indirectly reflect the variations of representative contaminants (phenols, etc.) in CWW. Therefore, it can be used as an integrated monitoring method for CWWTPs operation. Further research can be focused on the tracking of CWW discharge along the river or lake based on these identified CDOM components.

Acknowledgments

This work was supported by the National Natural Science Foundation of China (Grant No. 51308224), the Joint Funds of the National Natural Science Foundation of China (Grant No. U1201234) and the China Postdoctoral Science Foundation (Grant No. 2012M521603).

Appendix A. Supplementary material

Supplementary data associated with this article can be found, in the online version, at http://dx.doi.org/10.1016/j.chemosphere.2014.04.102.

References

Akcil, A., Karahan, A., Ciftci, H., Sagdic, O., 2003. Biological treatment of cyanide by natural isolated bacteria (*Pseudomonas* sp.). Miner. Eng. 16, 643–649.
Alarcón, F., Báez, M.E., Bravo, M., Richter, P., Escandar, G.M., Olivieri, A.C., Fuentes, E., 2012. Feasibility of the determination of polycyclic aromatic hydrocarbons in edible oils *via* unfolded partial least-squares/residual bilinearization and parallel factor analysis of fluorescence excitation emission matrices. Talanta 103, 361–370.
Angelino, S., Gennaro, M., 1997. An ion-interaction RP-HPLC method for the determination of the eleven EPA priority pollutant phenols. Anal. Chim. Acta 346, 61–71.
APHA, 1998. Standard Methods for the Examination of Water and Wastewater. American Public Health Association, Washington, DC.
Baker, A., Inverarity, R., Charlton, M., Richmond, S., 2003. Detecting river pollution using fluorescence spectrophotometry: case studies from the Ouseburn, NE England. Environ. Pollut. 124, 57–70.
Bridges, J., Williams, R., 1968. The fluorescence of indoles and aniline derivatives. Biochem. J. 107, 225–237.
Bro, R., 1997. PARAFAC. Tutorial and applications. Chemometr. Intell. Lab 38, 149–171.
Burich, I., Nikolich, K., Aleksich, A., 1974. Fluorescence of the hydrochlorides of some quinoline derivatives. J. Appl. Spectrosc. 21, 1200–1204.
Coble, P.G., 1996. Characterization of marine and terrestrial DOM in seawater using excitation–emission matrix spectroscopy. Mar. Chem. 51, 325–346.
Hoge, F.E., Vodacek, A., Swift, R.N., Yungel, J.K., Blough, N.V., 1995. Inherent optical properties of the ocean: retrieval of the absorption coefficient of chromophoric dissolved organic matter from airborne laser spectral fluorescence measurements. Appl. Opt. 34, 7032–7038.
Hua, B., Veum, K., Yang, J., Jones, J., Deng, B., 2010. Parallel factor analysis of fluorescence EEM spectra to identify THM precursors in lake waters. Environ. Monit. Assess. 161, 71–81.
Hudson, N., Baker, A., Reynolds, D., 2007. Fluorescence analysis of dissolved organic matter in natural, waste and polluted waters—a review. River Res. Appl. 23, 631–649.
Kim, Y.M., Park, D., Lee, D.S., Jung, K.A., Park, J.M., 2009. Sudden failure of biological nitrogen and carbon removal in the full-scale pre-denitrification process treating cokes wastewater. Bioresource Technol. 100, 4340–4347.
Kowalczuk, P., Durako, M.J., Young, H., Kahn, A.E., Cooper, W.J., Gonsior, M., 2009. Characterization of dissolved organic matter fluorescence in the South Atlantic Bight with use of PARAFAC model: interannual variability. Mar. Chem. 113, 182–196.
Li, W.H., Sheng, G.P., Liu, X.W., Yu, H.Q., 2008. Characterizing the extracellular and intracellular fluorescent products of activated sludge in a sequencing batch reactor. Water Res. 42, 3173–3181.
Lu, R., Sheng, G.P., Liang, Y., Li, W.H., Tong, Z.H., Chen, W., Yu, H.Q., 2013. Characterizing the interactions between polycyclic aromatic hydrocarbons and fulvic acids in water. Environ. Sci. Pollut. R. 20, 2220–2225.

Maranon, E., Vazquez, I., Rodriguez, J., Castrillon, L., Fernandez, Y., Lopez, H., 2008. Treatment of coke wastewater in a sequential batch reactor (SBR) at pilot plant scale. Bioresource Technol. 99, 4192–4198.

Ministry of Environmental Protection, P., 2012. Emission Standard of Polutants for Coking Chemical Industry. Peking, China (in Chinese).

Mounier, S., Patel, N., Quilici, L., Benaim, J.Y., Benamou, C., 1999. Three-dimensional fluorescence of the dissolved organ carbon in the Amazon River. Water Res. 33, 1523–1533.

NDRC, 2006. The Pollution and Suggestion in Coking Industries. <http://www.ndrc.gov.cn/gzdt/t20060907_83519.htm>.

Ou, H.S., Wei, C.H., Deng, Y., Gao, N.Y., 2013. Principal component analysis to assess the composition and fate of impurities in a large river-embedded reservoir: Qingcaosha Reservoir. Environ. Sci. Proc. Impact 15, 1613–1621.

Staib, C., Lant, P., 2007. Thiocyanate degradation during activated sludge treatment of coke-ovens wastewater. Biochem. Eng. J. 34, 122–130.

Wei, X.X., Zhang, Z.Y., Fan, Q.L., Yuan, X.Y., Guo, D.S., 2012. The effect of treatment stages on the coking wastewater hazardous compounds and their toxicity. J. Hazard. Mater. 239–240, 135–141.

Wu, J., Zhang, H., He, P.J., Shao, L.M., 2011. Insight into the heavy metal binding potential of dissolved organic matter in MSW leachate using EEM quenching combined with PARAFAC analysis. Water Res. 45, 1711–1719.

Yang, W.L., Li, X.C., Pan, B.C., Lu, L., Zhang, W.M., 2013. Effective removal of effluent organic matter (EfOM) from bio-treated coking wastewater by a recyclable aminated hyper-cross-linked polymer. Water Res. 47, 4730–4738.

Yao, X., Zhang, Y., Zhu, G., Qin, B., Feng, L., Cai, L., Gao, G., 2011. Resolving the variability of CDOM fluorescence to differentiate the sources and fate of DOM in Lake Taihu and its tributaries. Chemosphere 82, 145–155.

Zhang, M., Tay, J.H., Qian, Y., Gu, X.S., 1998. Coke plant wastewater treatment by fixed biofilm system for COD and NH_3-N removal. Water Res. 32, 519–527.

Zhang, W., Wei, C., Peng, P., Ren, M., 2010. Components and degradation characteristics analysis of phenols in coking wastewater in biological fluidized bed A/O/O process. Chin. J. Environ. Eng. 2, 253–258 (in Chinese).

Zhang, W., Wei, C., Yan, B., Feng, C., Zhao, G., Lin, C., Yuan, M., Wu, C., Ren, Y., Hu, Y., 2013. Identification and removal of polycyclic aromatic hydrocarbons in wastewater treatment processes from coke production plants. Environ. Sci. Pollut. R. 20, 6418–6432.

Zhao, W., Huang, X., Lee, D., 2009. Enhanced treatment of coke plant wastewater using an anaerobic–anoxic–oxic membrane bioreactor system. Sep. Purif. Technol. 66, 279–286.